Decreased fatty acid esterification compensates for the reduced lipolytic activity in hormone-sensitive lipase-deficient white adipose tissue

Robert Zimmermann,[1,*] Guenter Haemmerle,[1,*] Elke M. Wagner,[*] Juliane G. Strauss,[*] Dagmar Kratky,[†] and Rudolf Zechner[2,*]

Institute of Molecular Biology, Biochemistry, and Microbiology,* and Institute of Medical Biochemistry and Medical Molecular Biology,† University of Graz, Graz, Austria

Abstract **It has been observed previously that hormone-sensitive lipase-deficient (HSL-ko) mice have reduced white adipose tissue (WAT) stores compared to control mice. These findings contradict the expectation that the decreased lipolytic activity in WAT of HSL-ko mice would cause accumulation of triglycerides (TGs) in that tissue. Here we demonstrate that the cellular TG synthesis in HSL-deficient WAT is markedly reduced due to downregulation of the enzymatic activities of glycerophosphate acyltransferase, dihydroxyacetonphosphate acyltransferase, lysophosphatidate acyltransferase, and diacylglycerol acyltransferase. Fatty acid de novo synthesis is also decreased due to reduced cellular glucose uptake, reduced glucose incorporation into adipose tissue lipids, and reduced activities of acetyl:CoA carboxylase and fatty acid synthase. Finally, the activities of phosphoenolpyruvate carboxykinase (PEPCK), acyl:CoA synthetase (ACS), and glucose 6-phosphate dehydrogenase, the enzymes that provide glycerol-3-phosphate, acyl-CoA, and NADPH for TG synthesis, respectively, are decreased in HSL-ko mice. The reduced expression of the peroxisome proliferator-activated receptor γ (PPARγ) target genes PEPCK, ACS, and aP2, as well as reduced mRNA levels of PPARγ itself, suggest the involvement of this transcription factor in the downregulation of lipogenesis. Taken together, these results establish that in the absence of HSL, the reduced NEFA production is counteracted by a drastic reduction of NEFA reesterification that provides sufficient quantities of NEFA for release into the circulation. These metabolic adaptations result in decreased fat mass in HSL-ko mice.**—Zimmermann, R., G. Haemmerle, E. M. Wagner, J. G. Strauss, D. Kratky, and R. Zechner. **Decreased fatty acid esterification compensates for the reduced lipolytic activity in hormone-sensitive lipase-deficient white adipose tissue.** ***J. Lipid Res.*** **2003.** 44: **2089–2099.**

Supplementary key words triglyceride synthesis • fatty acid synthesis • peroxisome proliferator-activated receptor γ

Manuscript received 7 May 2003 and in revised form 4 August 2003.

Published, JLR Papers in Press, August 16, 2003.
DOI 10.1194/jlr.M300190-JLR200

Storage and mobilization of metabolic energy in mammals are coordinated by tight hormonal control of the synthesis and the catabolism of triglycerides (TGs) in white adipose tissue (WAT). Imbalances in these anabolic and catabolic processes might be involved in dysregulation of body weight control and the pathogenesis of obesity and related disorders. Hormone-sensitive lipase (HSL) is considered to be the central enzyme in the mobilization of WAT-TG stores. This multifunctional enzyme has been shown to hydrolyse TGs, diglycerides, and monoglycerides, as well as cholesteryl ester and other small water-soluble substrates (1). During periods of increased energy demand, HSL is activated by hormones such as catecholamines, which leads to an increase in the intracellular cAMP levels, resulting in the activation of protein kinase A (PKA) and phosphorylation of HSL (2). In parallel, activation of PKA leads to the phosphorylation of perilipin A, which elicits the translocation of phosphorylated HSL from the cytoplasm to the lipid droplet (3), a process that might also involve lipotransin (4). Once activated and translocated, HSL can hydrolyze lipid droplet-associated TG, and the mobilized nonesterified fatty acids (NEFAs) are released from WAT into the circulation.

Hormone-sensitive lipase-deficient (HSL-ko) mice exhibited a marked decrease of acylglyceride hydrolase activity in WAT, mainly because of decreased diglyceride hydrolase

Abbreviations: ACC, acetyl-CoA carboxylase; ACS, acyl-CoA-synthetase; aP2, adipocyte fatty acid binding protein; DGAT, diacylglycerol acyltransferase; FAS, fatty acid synthase; G6PDH, glucose-6-phosphate dehydrogenase; GNPAT, glycerophosphate acyltransferase; GPAM, mitochondrial GPAT; GPAT, glycerol-3-phosphate acyltransferase; HSL, hormone-sensitive lipase; LPAAT, lysophosphatidate acyltransferase; PEPCK, phosphoenolpyruvate carboxykinase; PL, phospholipid; PPAR, peroxisome proliferator-activated receptor; SREBP, sterol regulatory element binding protein; TG, triglyceride; WAT, white adipose tissue.

[1] R. Zimmerman and G. Haemmerle contributed equally to this study.
[2] To whom correspondence should be addressed.
e-mail: rudolf.zechner@kfunigraz.ac.at

activity (5). Accordingly, fasted HSL-ko mice had reduced plasma NEFA and TG levels, and liver TG stores were depleted, indicating that under starving conditions, the HSL-ko WAT is not able to supply the body with sufficient NEFA (6). In the fed state, HSL-ko mice have normal NEFA and TG levels in plasma, and experiments with ex vivo fat pads and isolated adipocytes showed that the basic NEFA release in HSL-ko cells is similar to that of controls and can be stimulated by β-adrenergic agonists (5, 7). Accordingly, at least one more as yet unidentified lipase(s), in addition to HSL, is thought to be present in adipose tissue (AT) (5, 7). However, this hypothetical lipolytic enzyme(s) cannot fully compensate for the absence of HSL, as evident from the reduced total acylhydrolase activity observed in HSL-ko mice (5, 8). Additionally, HSL-ko mice exhibited reduced WAT mass (9). This unexpected finding indicated that in addition to HSL-independent lipolytic activities, other metabolic adaptations must exist that affect TG synthesis in HSL-deficient WAT. Therefore it is conceivable that a reduction of NEFA re-esterification could cause reduced fat synthesis, thereby increasing the NEFA supply for the vascular system.

In this study, we demonstrate that in the absence of HSL, the esterification of NEFA is drastically reduced, leading to TG resynthesis and providing a compensatory mechanism for the reduced lipolytic activity. Together with the observed decrease in de novo synthesis of fatty acids, the downregulation of TG synthesis also provides a plausible explanation for the observed loss in WAT mass in HSL-ko mice.

EXPERIMENTAL PROCEDURES

Animals

HSL-ko mice were generated by targeted homologous recombination as previously described (5). For breeding experiments, mice heterozygous for the deleted HSL allele were used to generate homozygous HSL-ko animals. Mice were maintained on a regular light-dark cycle (14 h light, 10 h dark) and kept on a standard laboratory chow diet (4.5% wt/wt fat). Only male animals at the age of 22 to 26 weeks were used for metabolic experiments. Blood samples and epididymal fat pads were collected from fed (ad libitum access to food overnight) or fasted (food was removed for 20 h) animals between 9 AM and 10 AM.

Primers and probes

cDNA probes for Northern blot analysis of mouse diacylglycerol acyltransferase-1 and -2 (DGAT-1, DGAT-2), mitochondrial glycerol-3-phosphate acyltransferase (GPAM), lysophosphatidate acyltransferase (LPAAT), glycerophosphate acyltransferase (GNPAT), acyl-CoA synthetase (ACS), and sterol regulatory element binding protein (SREBP) were prepared by RT-PCR by using first-strand cDNA from mouse fat mRNA. The PCR primers used to generate these probes were as follows. *DGAT-1*: forward, 5′-TCT GAG GTG CCA TCG TCT GC-3′, and reverse, 5′-CGG CAC CAC AGG TTG ACA TC-3′; *DGAT-2*: forward, 5′-TGG CTC CAG CAT CCT CTC AG-3′, and reverse, 5′-AGA TCA GCT CCA TGG CGC AG-3′; *GPAM*: forward, 5′-ATT CCT GCA CGC CAC AGA GC-3′, and reverse, 5′-TGA TAA CGC CTC TCG CCA CA-3′; *LPAAT*: forward, 5′-AGA GAT ACA GCC AGC CGC CA-3′, and reverse, 5′-CCG GAA GAT GGT GAG CAT GG-3′; *GNPAT*: forward, 5′-CGC ATA GGA GCC ATT CGG TT-3′, and reverse, 5′-AGT GGT GGA CTC CTT CGG CT-3′; *ACS*: forward, 5′-GAA GAT CAA GCG AGG CTC CA-3′, and reverse, 5′-CCT TCC TGC ATT CCA TCG TC-3′; *SREBP-1*: forward, 5′-GCAAATCACT-GAAGGACCTGG-3′, and reverse, 5′-GCTGGTGCAGCTTATGG-TAGAC-3′. A 977 bp XhoI fragment derived from the cytosolic isoform of mouse phosphoenolpyruvate carboxykinase (PEPCK) cDNA was used to detect PEPCK mRNA. The cDNA-specific PCR products containing single 3′-dA overhangs generated by Taq polymerase (AdvanTaq DNA polymerase, Clontech) were cloned into the linearized acceptor vector pST-Blue-1 (Novagen, Madison, WI).

The following primer sequences specific for β-actin, glucose-6-phosphate dehydrogenase (G6PDH), and fatty acid synthase (FAS) were used for real-time PCR. β-actin: forward, 5′-GAC AGG ATG CAG AAG GAG ATT ACT G-3′, and reverse, 5′-GCC ACC GAT CCA CAC AGA GT-3′, probe 5′-CAA GAT CAT TGC TCC TCC TGA GCG CA-3′; *G6PDH*: forward, 5′-GGG CAA AGA GAT GGT CCA GA-3′, and reverse, 5′-CAA TGT TGT CTC GAT TCC AGA TG-3′, probe 5′-ATC CTG TTG GCA AAC CTC AGC ACC A-3′; *FAS*: forward, 5′-ATG TGA ACA GCG CAG GCA C-3′, and reverse, 5′-ACA ATG CCC ACG TCA CCA AT-3′, probe 5′-TGT CCT CCC AGG CCT TGC CGT-3′.

Tissue preparation and enzyme assays

For measurement of AT and ACS activity, intraperitoneal fat pads were surgically removed and washed in PBS containing 1 mM EDTA. Homogenization was performed on ice in lysis buffer (0.25 M sucrose, 1 mM EDTA, 1 mM dithioerythritol) using a motor-driven teflon glass homogenizer (8 strokes at medium speed; Schütt Labortechnik, Germany). The homogenized tissue was centrifuged at 1,000 *g* for 15 min. The supernatant was centrifuged at 100,000 *g* to obtain membrane and cytosolic fractions. For photometric assays of acetyl-CoA carboxylase (ACC), FAS, and G6PDH, fat pad homogenates were prepared as follows. Abdominal fat pads were shock frozen in liquid nitrogen and homogenized in 3 vol of cold homogenization buffer [9 mM KH_2PO_4, 85 mM K_2HPO_4, 1 mM DTT, and 70 mM $KHCO_3$, (pH 7)]. After centrifugation for 12 min at 20,000 *g*, the fat cake was discarded, and the cytosolic fraction was obtained after centrifugation of the supernatant at 100,000 *g* for 1 h at 4°C.

ACS activity was measured as synthesis of acyl-CoA in the presence of 2 mM [^{3}H]9,10-oleic acid (3,000 cpm/nmol) and 0.6 mM CoA as described (10). The reaction was performed in a volume of 0.2 ml and contained 0.1 M Tris-HCl (pH 8), 5 mM DTT, 0.15 M KCl, 15 mM $MgCl_2$, 15 mM ATP, and 5 μg protein of the membrane fraction. The mixture was incubated for 10 min at 37°C, and the reaction was stopped by the addition of 2.25 ml isopropanol-hexane-1 M H_2SO_4 (40:10:1; v/v/v). After centrifugation (5 min, 1,000 *g*), the upper phase was removed, and the lower phase containing the water-soluble acyl-CoA was washed twice with hexane containing 4 mg/ml oleic acid. The radioactivity in the aqueous phase was determined by liquid scintillation.

Glycerol-3-phosphate acyltransferase (GPAT) and GNPAT activities were measured as described by Jones and Hajra (11) using ^{32}P-labeled glycerol-3-phosphate or dihydroxyacetone phosphate (500 cpm/nmol) and palmitoyl-CoA as substrate. The reaction was performed in a volume of 0.6 ml and contained 5 μg cell membrane protein, 75 mM Tris-HCl, pH 7.5 (for GPAT activity), or 2-[*N*-morpolino]ethansulfonic acid, pH 5.5, (for GNPAT activity), 1.7 mg/ml BSA, 8.3 mM NaF, 8.3 mM $MgCl_2$, 83 μM palmitoyl-CoA, 420 μM ^{32}P-labeled glycerol or dihydroxyacetone, and 100 μl of an egg yolk-lecithin suspension (Sigma P7318, 20 mg/ml) prepared by sonification in 10 mM Tris-HCl (pH 7.5) and 1 mM EDTA and centrifuged at 40,000 *g* for 30

min. To distinguish between mitochondrial and microsomal GPAT activity (GPAM and GPATer, respectively), the membrane proteins were incubated in the absence or in the presence of 2 mM *N*-ethylmaleimide for 15 min on ice (12). After incubation for 10 min at 37°C, the reaction was stopped by the addition of 2.25 ml $CHCl_3$-methanol (1:2; v/v). Phase separation was achieved by the addition of 0.75 ml $CHCl_3$ and 0.75 ml 2 M KCl in 0.2 M H_3PO_4. After centrifugation (5 min, 1,000 *g*), the upper phase was removed, and the organic phase was washed twice with chloroform-methanol-0.5 N H_3PO_4 (1:12:12; v/v/v). The radioactivity in the organic phase was determined by liquid scintillation.

LPAAT activity was measured with 1-oleoyl-*sn*-glycero-3-phosphate as acceptor and [1-^{14}C]palmitoyl-CoA as acyl donor (25,000 cpm/nmol) as described (13). The reaction mixture contained 0.1 M Hepes (pH 7.5), 0.2 M NaCl, 5% glycerol, 10 mM EDTA, 5 mM β-mercaptoethanol, 20 μM lysophosphatidate (LPA), 40 μM acyl-CoA, and 5 μg cell membrane protein in a volume of 0.2 ml. After incubation for 10 min at 37°C, the lipids were extracted as described (14). The organic phase was dried in a SpeedVac concentrator, redissolved in $CHCl_3$ containing phosphatidic acid as standard, and applied onto TLC plates (Silica gel 60, plastic, VWR). The TLC plates were developed in $CHCl_3$-methanol-water (65:25:4; v/v/v). The lipids were visualized with iodine vapor, the radioactive spots corresponding to phosphatidic acid were cut out, and the radioactivity was quantitated by liquid scintillation.

DGAT activities were determined as described (15), with *sn*-1,2-dioleoylglycerol as acceptor and 1-[^{14}C]palmitoyl-CoA as acyl donor (25,000 cpm/nmol). The reaction mixture contained 175 mM Tris-HCl (pH 8), 1 mg/ml BSA (fatty acid-free), 16 mM $MgCl_2$, 0.2 mM diacylglycerol, 40 μM palmitoyl-CoA, and 5 μg cell membrane protein in a volume of 0.2 ml. The reaction mixture was incubated for 10 min at 25°C. The lipids were extracted as described (14), dried, redissolved in $CHCl_3$ containing trioleylglycerol as standard, and applied to TLC plates. The TLC plates were developed in hexan-diethylether-acetic acid (70:29:1; v/v/v). Visualization and quantitation of the radioactive TG spots were performed as described above.

ACC activity was measured using an NADH-linked assay, with slight modifications (16). The medium [56 mM Tris-HCl (pH 8), 10 mM $MgCl_2$, 11 mM EDTA, 4 mM ATP, 52 mM $KHCO_3$, 0.75 mg/ml BSA, 0.5 mM NADH, 1.4 mM phosphoenolpyruvate] was mixed with 5.6 U/ml pyruvate kinase and 5.6 U/ml lactate dehydrogenase. The baseline was followed at 30°C until a constant slope was reached. Per 170 μl medium, 75 μl of activated homogenate was added, and the reaction was started with acetyl-CoA (0.125 mM final concentration). For enzyme activation, 1 vol homogenate was incubated with 1 vol activation buffer [20 mM citrate, 100 mM Tris-HCl (pH 8), 1.5 mg/ml BSA, 20 mM $MgCl_2$, and 20 mM GSH (pH 7.5)] for 15 min at 37°C.

FAS activity was determined as the decrease of the NADPH absorption at 340 nm as described earlier (17). G6PDH was investigated following the increase of NADPH absorption at 340 nm. For detecting G6PDH, a medium containing 50 mM Tris buffer (pH 8), 1 mM $MgCl_2$, and 5 mM NADP was mixed with 60 μg cytosolic protein/ml, and the reaction was started with glucose-6-phosphate (8 mM final concentration) at 37°C.

Determination of WAT NEFA levels

WAT was surgically removed, extensively washed with ice-cold PBS, and extracted as described (14) under acidic conditions (0.1% acidic acid). An aliquot of the extract was dried in a SpeedVac concentrator, and the NEFA content was determined using a commercial kit (Wako Chemicals, Germany).

In vitro incorporation of NEFA into TGs and phospholipids of ex vivo fat pads

Pieces of intraperitoneal WAT (30–40 mg) were incubated in DMEM medium containing 1% BSA (NEFA-free) for 6 h at 37°C in the presence of 200 μM oleic acid (5 μCi/well [^{3}H]9,10-oleic acid). The lipids were extracted as described (14). An aliquot of the lipid extract was analyzed by TLC using hexan-diethylether-acetic acid (70:29:1; v/v/v) as mobile phase. The lipids were visualized with iodine vapor, and the radioactive spots corresponding to TG and phospolipids (PLs) were cut out and quantitated by liquid scintillation.

Uptake of 2-deoxy-[1-^{3}H]D-glucose and incorporation of D-[^{14}C]glucose into the lipid moiety in ex vivo fat pads

For measurement of [^{3}H]deoxyglucose uptake, fat pads (30–40 mg) were incubated for 30 min at 37°C in Krebs-Ringer buffer (pH 7.4) containing 1% BSA and 1 μCi/ml [^{3}H]deoxyglucose. Thereafter, the fat pads were extensively washed and digested in lysis buffer A containing 1% SDS, 400 μg/ml proteinase K, 100 mM NaCl, 10 mM Tris (pH 7.5), and 1 mM EDTA. Aliquots of the lysate were used for determination of radioactivity and quantitation of DNA. To measure D-glucose incorporation into the lipid moiety, pieces of intraperitoneal WAT (30–40 mg) were incubated in DMEM medium containing 1 g/l D-glucose, 1% BSA (NEFA-free), and 0.5 μCi/ml D-[^{14}C]glucose for 6 h at 37°C. Lipids were extracted from fat pads as described (14), and the organic phase was washed two times and dried under nitrogen. TLC analysis was performed as described above. The spots corresponding to PL, NEFA, and TG were cut out and quantitated by liquid scintillation. For determination of incorporation of D-glucose into TG-associated fatty acids (TG-NEFAs), the lipid extracts were digested with a TG lipase from *Candida rugosa* (4 U/ml, Sigma Chemicals Co.) for 3 h at 37°C, and the released fatty acids were separated by TLC.

In vivo uptake of 2-deoxy-[1-^{3}H]D-glucose and incorporation of D-[^{14}C]glucose into TGs of WAT

Fed mice were injected intraperitoneally with a solution containing 0.15 M NaCl, 100 mg/ml D-glucose, 4 μCi/ml [^{3}H]deoxyglucose, and 4 μCi/ml D-[^{14}C]glucose (18 μl/g mouse). After 2 h, mice were sacrificed, and pieces of the gonadal fat pads were extensively washed in PBS containing 0.01% EDTA. For determination of [^{3}H]deoxyglucose uptake and quantitation of DNA, the fat pads were lysed in lysis buffer A as described above. For measurement of D-[^{14}C]glucose incorporation into WAT lipids, fat pads were extracted as described (14) and subsequently lysed in lysis buffer A for DNA determination. Aliquots of the WAT lysate and of the lipid extract were quantitated by liquid scintillation.

Determination of WAT DNA content and protein determinations

WAT DNA was isolated by overnight digestion in lysis buffer A and precipitated in ethanol. The tissue DNA content was quantitated fluorimetrically by the method of Labarca and Paigen (18). Protein concentrations were measured with the BCA reagent (Pierce) using bovine albumin as standard.

Northern blot analysis and real-time PCR

Total RNA was isolated from WAT using the TRI Reagent procedure according to manufacturer's protocol (Molecular Research Center, Karlsruhe, Germany). Specific mRNAs were detected using standard Northern blotting techniques with 10 μg total RNA (19). Probes for specific hybridization were generated

JOURNAL OF LIPID RESEARCH ASBMB

using random priming. Northern blots were visualized by exposure to a PhosphorImager Screen (Apbiotech, Freiburg, Germany) and analyzed using ImageQuant software. Quantitative real-time PCR analysis was used to determine the relative levels of ACC, G6PDH, PEPCK, and PDH. Reverse transcription and PCR were performed according to the manufacturer's instructions (TaqMan™ One-step RT-PCR Kit, Applied Biosystems, Vienna, Austria) on the 5700 AbiPrism Sequence Detection System (Applied Biosystems). Primers and TaqMan™ probes were designed using Primer Express software (Applied Biosystems) and excluded detection of genomic DNA. Sequence-specific amplification was detected with an increasing fluorescence signal, with FAM as the reporter dye, during the amplification cycle. Amplification of murine β-actin was performed on all samples tested as an internal control for variations in RNA amounts. Levels of the different mRNAs were subsequently normalized to β-actin mRNA levels.

Western blotting

For the preparation of protein extracts, epididymal WAT was homogenized in a buffer containing 1% SDS, 1% Triton X-100, 50 mM Tris-HCL (pH 7.4), 5 mM EDTA, 15 U/ml DNase I (Boehringer Mannheim, Inc.), 1× complete protease inhibitor cocktail (Roche Diagnostics Inc., Germany). Proteins (20 μg) were separated by SDS-PAGE and transferred to a nitrocellulose membrane (Schleicher and Schuell, Inc.). Blots were incubated with 1:300-diluted affinity-purified rabbit polyclonal antibody raised against SREBP-1 p125 and p68 (SREBP-1, K-10; Santa Cruz Biotechnology, Inc.). Bound immunoglobulins were detected with a horseradish peroxidase anti-rabbit IgG conjugate (Vector Laboratories) and visualized by enhanced chemiluminescence detection (Amersham Biosciences) according to the manufacturers' instructions.

RESULTS

Body weight and WAT mass of HSL-ko and control mice

The effects of HSL deficiency on body mass composition was analyzed by the determination of total body weight and AT mass from several fat depots. No significant differences were found in body weight of male and female HSL-ko mice compared with control mice (**Table 1**). In contrast, gonadal WAT mass was significantly reduced in 15–18-week-old female mice (−30%). Gonadal fat mass was even more decreased in older mice. At the age of 40–45 weeks, female and male mice exhibited a 70% and 71% reduction, respectively. In histological examinations, epididymal WAT of HSL-ko and control mice appeared as unilocular AT with a large single lipid droplet in mature adipocytes. By visual inspection, the cell size of adipocytes appeared much more heterogeneous in HSL-ko mice than in control animals (not shown). Although an extensive morphometric analysis to determine the mean cell size was not performed, the tissue mass per μg DNA was decreased by 46% ($n = 5$; $P < 0.05$) in HSL-ko mice, suggesting a reduced mean size of adipocytes.

Tissue NEFA levels of HSL-ko WAT

In a previous study, we demonstrated that despite decreased lipolytic activity, HSL-ko fat pads exhibited a basic NEFA release, which can be stimulated by isoproterenol, similar to that of controls (5). The determination of intracellular steady-state NEFA levels revealed identical results in nonstimulated fat pads of HSL-ko mice and control animals (**Fig. 1**). After stimulation of lipolysis for 1 h with isoproterenol, increased steady-state NEFA levels were observed (3.3- and 5.3-fold in HSL-ko and control WAT, respectively), suggesting that cellular mechanisms exist that enable the HSL-ko WAT to maintain normal tissue NEFA levels despite the reduced lipolytic activity.

In vitro incorporation of free fatty acid into the lipid moiety in WAT

To assess whether decreased fatty acid esterification and synthesis of TG and PL are responsible for the maintenance of normal steady-state NEFA concentrations in HSL-deficient WAT, the incorporation of [^{3}H]9,10-oleic acid into the lipid moiety was measured in ex vivo fat pads from control and HSL-ko mice. As shown in **Fig. 2A**, the incorporation of radioactivity into TG was 6-fold and 19-fold higher in fed than in fasted WAT of control and HSL-ko mice, respectively. Additionally, HSL-ko mice exhibited a reduced esterification capacity to produce WAT-TG compared with control mice under both nutritional conditions (−51% in fed mice and −84% in fasted mice). The incorporation of NEFA into PL was much less affected by the nutritional condition than was its incorporation into TG. Whereas fasted control animals exhibited a 39% reduction of PL formation in fat pads, PL formation in HSL-deficient WAT was unaffected by the nutritional state. The effect of the genotype on the incorporation of NEFA into PL, however, was still significant. In fed HSL-ko

TABLE 1. Body weight and gonadal WAT mass of control (wt) and HSL-ko animals

Age, Gender	wt (n)	HSL-ko (n)	*t*-test
Body weight (g)			
15–18 Weeks, female	29.2 ± 1.9 (8)	30.7 ± 2.1 (8)	ns
40–45 Weeks, female	29.8 ± 5.8 (8)	30.0 ± 3.9 (8)	ns
40–45 Weeks, male	35.7 ± 2.8 (9)	35.8 ± 3.2 (11)	ns
Gonadal WAT mass (% of body weight)			
15–18 Weeks, female	1.21 ± 0.23 (8)	0.85 ± 0.20 (8)	$P < 0.05$
40–45 Weeks, female	4.26 ± 1.21 (8)	1.25 ± 0.39 (8)	$P < 0.001$
40–45 Weeks, male	1.98 ± 0.71 (9)	0.57 ± 0.28 (11)	$P < 0.001$

HSL, hormone-sensitive lipase; HSL-ko, hormone-sensitive lipase-deficient; ns, nonsignificant; WAT, white adipose tissue; wt, wild-type. Animals used for this study were littermates and were kept on a standard laboratory chow diet (4.5% wt/wt fat). Data are expressed as means ± SD.

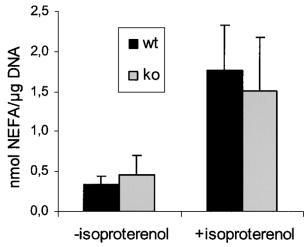

Fig. 1. Tissue nonesterified fatty acid (NEFA) levels in white adipose tissue (WAT) of wild-type (wt) and knockout (ko) animals. Gonadal fat pads were surgically removed from fed mice and incubated in DMEM containing 1% BSA (NEFA-free) for 1 h in the presence or in the absence of 10 µM isoproterenol. Lipids were extracted as described under Experimental Procedures. Data are expressed as mean ± SD (n = 10 for each group).

mice, PL formation was reduced by 56% compared with control animals. After fasting, HSL-ko mice exhibited a 30% reduction.

Activity and mRNA levels of NEFA-esterifying enzymes

The major enzymes involved in fatty acid esterification were analyzed on the levels of enzyme activities and mRNA concentrations. As shown in **Table 2**, in the fed state, the activity of ACS was decreased by 64% in HSL-ko mice compared with controls. The activities for GPAT, GNPAT, LPAAT, and DGAT were also significantly reduced, by 77%, 32%, 76%, and 85%, respectively. The decrease in GPAT activity was due to downregulation of both of the enzymes responsible for the *N*-ethylmaleimide-sensitive and -resistant activity corresponding to the cytoplasmatic and mitochondrial forms of GPAT activity. During fasting, all activities except LPAAT and ACS activity were drastically reduced in WAT of control animals, whereas in WAT of HSL-ko mice, the changes were much less pronounced. Accordingly, the enzyme activities in fasted wild-type and HSL-ko mice were identical for GPAT, GPAM, and GNPAT. In contrast, enzyme activities for ACS (−60%), LPAAT (−45%), and DGAT (−47%) were still

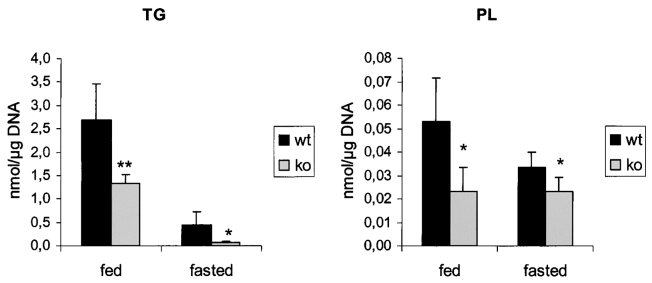

Fig. 2. Incorporation of NEFA into triglyceride (TG) and phospholipid (PL) into ex vivo fat pads of fed and fasted animals. Gonadal WAT (30–40 mg) from hormone-sensitive lipase-deficient [HSL-ko (ko)] and control [wild-type (wt)] mice was incubated in DMEM medium containing 1% BSA for 6 h at 37°C in the presence of 200 µM oleic acid (5 µCi/ml [^{3}H]9,10-oleic acid). Thereafter, lipids were extracted and separated by TLC as described under Experimental Procedures. Data are expressed as mean ± SD. (n = 5 for each group; * $P < 0.05$; ** $P < 0.01$, compared with wt).

significantly lower in WAT of fasted HSL-ko mice. To determine mRNA levels for the enzymes involved in the esterification of fatty acids, Northern blot analysis was performed in WAT from fed animals, with specific probes for mouse DGAT-1, DGAT-2, GPAM, LPAAT, and GNPAT. Significant changes in mRNA levels were found for GPAM, GNPAT, and DGAT-1 (−82%, −54%, and −88%, respectively) (**Fig. 3**). LPAAT and DGAT-2 showed a nonsignificant trend toward decreased mRNA levels (−23%, $P = 0.08$ and −53%; $P = 0.07$, respectively).

Uptake of 2-deoxy-[1-^{3}H]D-glucose and incorporation of D-glucose-associated ^{14}C into the lipid moiety of WAT fat pads

An alternative pathway to the maintenance of normal steady-state NEFA levels in lipolysis-defective WAT is provided by the increased de novo synthesis of fatty acids. Accordingly, we investigated whether HSL deficiency has an effect on the in vitro uptake of glucose and the incorporation of D-glucose into the lipid moiety of WAT. As shown in **Fig. 4A**, the uptake of 2-deoxy-[1-^{3}H]D-glucose was decreased by 39% in HSL-ko WAT. Additionally, the incorporation of D-glucose-associated ^{14}C into total lipids, TG, and PLs was also decreased by 67%, 66%, and 60%, respectively, in HSL-deficient WAT compared with control WAT (Fig. 4B). The radioactivity in TG-NEFAs was decreased by 94%, indicating that the de novo synthesis of fatty acids from glucose and NEFA esterification was drastically reduced. No significant differences were found for intracellular NEFA and released NEFA.

Uptake of 2-deoxy-[1-^{3}H]D-glucose and incorporation of D-glucose-associated ^{14}C into the lipid moiety of WAT in vivo

To verify the in vitro uptake and incorporation data from isolated fat pads in whole-animal experiments, 2-deoxy-[1-^{3}H]D-glucose and D-[^{14}C]glucose were injected into HSL-ko and control mice as described under Experimental Procedures. As shown in **Fig. 5**, accumulation of 2-deoxy-[1-^{3}H]D-glucose was decreased by 50%, and the incorporation of D-glucose-associated ^{14}C into the lipid moiety was reduced by 72% in HSL-ko WAT compared with control WAT. Taken together, these data suggest that the WAT of HSL-ko mice absorbs lower amounts of D-glucose and produces decreased amounts of lipids from D-glucose, compared with control WAT.

Activity and mRNA levels of enzymes implicated in fatty acid synthesis

Additional evidence for decreased de novo fatty acid synthesis in HSL-deficient WAT was obtained from the analysis of the involved enzyme activities and mRNA levels. As shown in **Table 3**, the activities of ACC, FAS, and G6PDH were decreased by 65%, 74%, and 38%, respectively, in HSL-ko WAT compared with control WAT. Accordingly, the mRNA levels for FAS and G6PDH were decreased by 85% and 58%, respectively (**Fig. 6**), suggesting that reduced NEFA synthesis was caused pri-

TABLE 2. Enzymatic activities of acyl-CoA synthetase and acyltransferases in WAT from fed and fasted animals

Enzyme	Fed Animals			Fasted Animals		
	wt (n = 5)	HSL-ko (n = 5)	*t*-test	wt (n = 4)	HSL-ko (n = 4)	*t*-test
	nmol/min/mg cell protein					
ACS	4.7 ± 0.5	1.7 ± 0.3	$P < 0.001$	4.2 ± 0.3	1.7 ± 0.4	$P < 0.001$
GPAT	14.5 ± 3.3	1.7 ± 0.5	$P < 0.001$	1.6 ± 0.4	2.0 ± 0.6	ns
GPATer	11.8 ± 2.4	1.1 ± 0.4	$P < 0.001$	1.0 ± 0.2	1.4 ± 0.3	ns
GPAM	2.8 ± 0.4	0.5 ± 0.1	$P < 0.01$	0.6 ± 0.4	0.6 ± 0.2	ns
GNPAT	2.5 ± 0.4	1.7 ± 0.5	$P < 0.05$	0.8 ± 0.3	1.2 ± 0.4	ns
LPAAT	7.0 ± 2.1	1.7 ± 0.5	$P < 0.01$	6.4 ± 1.2	3.5 ± 1.3	$P < 0.05$
DGAT	13.7 ± 1.5	2.1 ± 0.6	$P < 0.001$	7.2 ± 2.1	3.8 ± 0.6 (n = 5)	$P < 0.001$

ACS, acyl-CoA-synthetase; DGAT, diacylglycerol acyltransferase; GNPAT, glycerophosphate acyltransferase; GPAM, mitochondrial GPAT; GPAT, glycerol-3-phosphate acyltransferase; GPATer, microsomal GPAT; LPAAT, lysophosphatidate acyltransferase. Each assay was performed with 5 μg membrane protein of WAT from fed or fasted mice as described under Experimental Procedures. GPATer and GPAM correspond to the *N*-ethylamide-sensitive and -resistant GPAT activity, respectively. Data are given as mean ± SD of values obtained from WAT preparations of single mice.

marily by the transcriptional downregulation of the involved enzymes.

Peroxisome proliferator-activated receptor γ and SREBP-1c expression in WAT of HSL-ko and controls

To gain information about the transcriptional mechanisms leading to the downregulation of fatty acid and lipid synthesis in HSL-ko WAT, we investigated the contribution of the transcription factors peroxisome proliferator-activated receptor γ (PPARγ) and SREBP-1 in these processes. Northern blot analysis revealed that the PPARγ mRNA level was decreased by 43% in WAT of HSL-ko mice (**Fig. 7**). Additionally, the mRNA concentrations of the PPARγ-regulated genes PEPCK, aP2, and ACS were also downregulated by 70%, 48%, and 63%, respectively, suggesting that PPARγ is involved in the observed changes in WAT lipid synthesis. In contrast, no significant differences were found for ADD1/SREBP-1c on the mRNA and protein levels (**Fig. 8**).

DISCUSSION

Lipid storage and fatty acid mobilization in AT are important metabolic processes in mammals to manage continuous energy supply during infrequent nutrient uptake. The major process to provide NEFA to the vascular system during fasting is the induction of TG lipolysis, and HSL is chiefly responsible for the hydrolysis of acylglycerides in fat cells. The enzyme is activated by phosphorylation in response to hormonal stimuli such as catecholamines and glucocorticoids (20). Genetically modified mice that

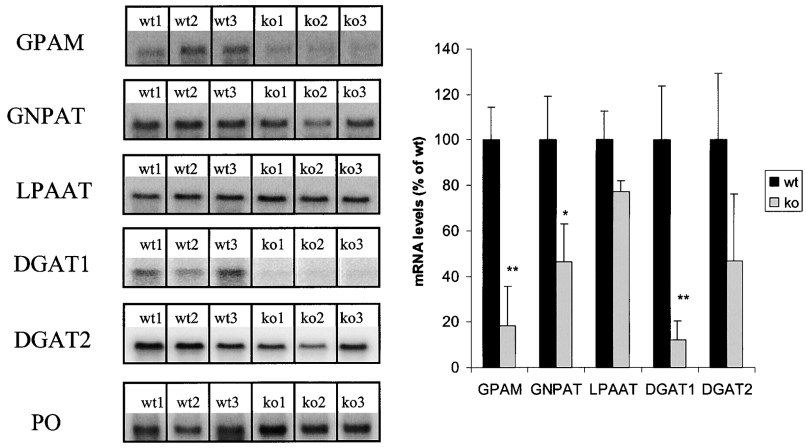

Fig. 3. Northern blotting analysis of acyltransferases (ATs) in WAT of wt and HSL-ko animals. Gonadal fat pads were surgically removed from fed mice, and total RNA (10 μg) was used for Northern blot analysis. Each lane corresponds to the RNA obtained from a single wt or HSL-ko mouse. The housekeeping gene for acidic ribosomal protein PO was used as internal standard. Northern blots were visualized by exposure to a PhosphorImager screen (Apbiotech) and analyzed using ImageQuant software. Data are expressed as mean ± SD. * $P < 0.05$; ** $P < 0.01$. GPAM, mitochondrial GPAT; GNPAT, glycerophosphate acyltransferase; LPAAT, lysophosphatidate acyltransferase; DGAT1, diacylglycerol acyltransferase-1; DGAT2, diacylglycerol acyltransferase-2.

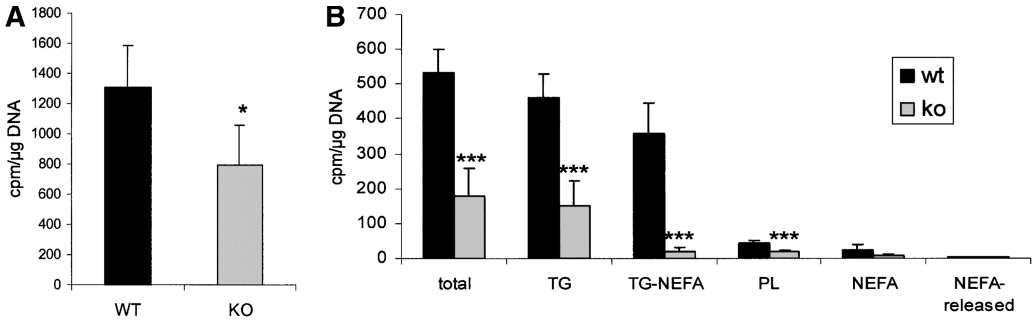

Fig. 4. Uptake of 2-deoxy-[1-^{3}H]D-glucose and incorporation of D-[^{14}C]glucose into the lipid moiety of ex vivo fat pads. A: For measurement of [^{3}H]deoxyglucose uptake, pieces of gonadal WAT (30–40 mg) from fed HSL-ko and control mice were incubated in Krebs-Ringer buffer containing 1% BSA and 1 µCi/ml [^{3}H]deoxyglucose for 30 min at 37°C. B: To determine the incorporation of D-[^{14}C]glucose into the lipid moiety, fat pads were incubated in DMEM medium containing 1% BSA, 1 g/l D-glucose, and 0.5 µCi/ml D-[^{14}C]glucose for 6 h at 37°C. Lipids were separated and quantitated as by TLC as described under Experimental Procedures. Data are expressed as mean ± SD (n = 5 for each group. * $P < 0.05$; *** $P < 0.001$).

lacked HSL exhibited reduced total acylglyceride hydrolase activity predominantly as a result of decreased diacylglyceride lipase activity (5). Unexpectedly, however, these animals did not increase their body weight or fat mass in response to HSL deficiency but exhibited decreased WAT depots, as observed in this study and by others (9). Decreased WAT mass was accompanied by a lower tissue mass-to-DNA ratio in HSL-deficient WAT, suggesting a smaller adipocyte size. Data on fat cell size in HSL-ko mice have been conflicting (8, 9); our data support the previous findings of Wang et al. (9) reporting smaller adipocyte size in response to HSL deficiency. In addition to the decreased fat mass, another unexpected finding was that plasma NEFA and TG levels in the fed state (6) and the rates of basal NEFA release (5, 9) were unchanged, compared with those of control mice. To test whether tissue NEFA levels are decreased in the case of HSL deficiency, we measured NEFA levels in WAT in the presence and in the absence of isoproterenol. Although not experimentally shown, we assume that in the WAT pieces, most of the fatty acids are intracellular and bound to fatty acid binding proteins such as aP2. Because HSL-deficient WAT exhibited NEFA levels similar to those of controls and was able to increase its NEFA levels in response to β-adrenergic stimulation, we suggest that HSL-deficient WAT is able to maintain normal cellular and plasma NEFA levels, as long as the mice are not extensively fasted (6).

To investigate the origin of adipocyte-associated NEFA, the metabolic processes that are involved in NEFA esterification and NEFA synthesis were analyzed. The results, summarized in **Fig. 9**, demonstrate that NEFA esterification pathways and the synthesis of neutral lipids and glycerol phospholipids are markedly decreased in HSL-ko mice, compared with controls, under both fed and fasted conditions. The enzyme activities of several acyltransferases (GPAT, GNPAT, LPAAT, and DGAT) and their corresponding mRNA levels were found to be reduced. Additionally, the activities and mRNA levels of the enzymes for providing acyl-CoA and glycerol-3-phosphate as precursors for glycerol-lipid synthesis were also reduced in HSL-ko mice. These data strongly support the notion that in a state of decreased lipolytic activity, as present in HSL-deficient WAT, normal NEFA levels are maintained by a drastic reduction in the (re-)esterification of NEFA. Kalderon et al. (21) stated that in fasted rat adipose tissue, two-thirds of the lipolyzed NEFA is actually re-esterified within a futile cycle and only one-third is released into the vascu-

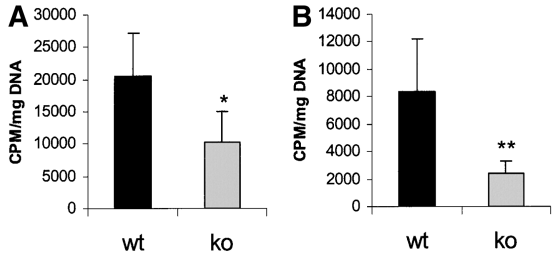

Fig. 5. In vivo incorporation of 2-deoxy-[1-^{3}H]D-glucose (A) and D-[^{14}C]glucose (B) into lipids of WAT of HSL-ko and wt mice. Fed mice were injected intraperitoneally with a solution containing 0.15 M NaCl, 100 mg/ml D-glucose, 2 µCi/ml [^{3}H]deoxyglucose, and 2 µCi/ml D-[^{14}C]glucose (18 µl/g mouse). After 2 h, mice were sacrificed, and pieces of the gonadal fat pads were removed. The tissue accumulation of [^{3}H]deoxyglucose and the incorporation of D-[^{14}C]glucose into lipids were determined as described under Experimental Procedures. (n = 6 for HSL-ko, and n = 5 for wt mice. * $P < 0.05$; ** $P < 0.01$.)

TABLE 3. Enzymatic activities of enzymes implicated in fatty acid synthesis

	Enzyme Activity		
	wt (n)	HSL-ko (n)	*t*-test
G6PDH IU/mg protein	348 ± 34 (6)	217 ± 61 (6)	$P < 0.01$
FAS IU/mg protein	2.8 ± 0.9 (6)	0.7 ± 0.2 (6)	$P < 0.001$
ACC IU/µg protein	53 ± 10 (3)	15 ± 12 (3)	$P < 0.05$

ACC, acetyl-CoA carboxylase; FAS, fatty acid synthase; G6PDH, glucose-6-phosphate dehydrogenase. Assays were performed with cytosolic proteins of WAT from fed mice. Catalytic enzyme activities were measured photometrically as described under Experimental Procedures. Data are given as mean ± SD of values obtained from WAT preparations of individual mice.

JOURNAL OF LIPID RESEARCH

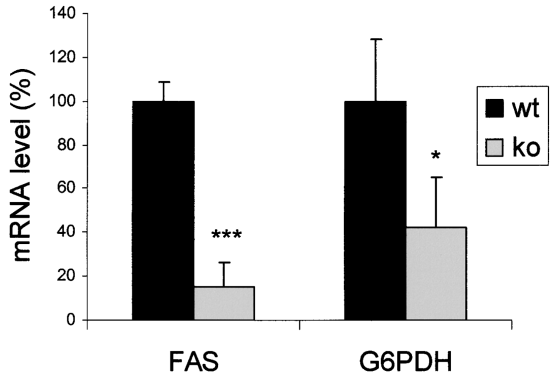

Fig. 6. Real-time PCR analysis of enzymes implicated in fatty acid synthesis. Gonadal fat pads were surgically removed from fed mice, and total RNA was isolated. Reverse transcription and PCR were performed according to the manufacturer's instructions (TaqMan™ One-step RT-PCR Kit, Applied Biosystems) on the 5700 Abi-Prism Sequence Detection System (Applied Biosystems). Amplification of murine β-actin was performed on all samples tested as an internal control for variations in RNA amounts. Levels of the different mRNAs were subsequently normalized to β-actin mRNA levels. (n = 6 for each group. * $P < 0.05$; *** $P < 0.001$.)

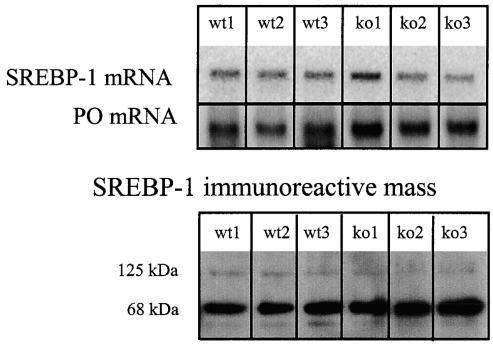

Fig. 8. SREBP-1 mRNA and protein analysis of WAT. Northern and Western blot analyses of SREB-1 in WAT of wt and HSL-ko mice. For Northern blotting, the gonadal fat pads were surgically removed from fed mice and total RNA was isolated. Each lane corresponds to the RNA obtained from a single wt or HSL-ko mouse. The housekeeping gene for acidic ribosomal protein PO was used as internal standard. For Western blotting analysis, 20 μg of total WAT protein from wt mice and ko mice was subjected to SDS-PAGE and electroblotted on nitrocellulose. SREBP-1 (125 kDa and 68 kDa) was detected with a polyclonal rabbit anti-SREBP-1 antiserum, with a horseradish peroxidase anti-rabbit IgG as secondary antibody.

lar system. Our results indicate that through inhibition of acyltransferases, the proportion of NEFA re-esterification versus NEFA secretion can be effectively changed in HSL-ko WAT, thereby providing a powerful regulatory system for NEFA export.

Our results are also in accordance with observations obtained in other mouse models and in vitro studies implying that acyltransferases and PEPCK are involved in adipose tissue development and in the regulation of NEFA mobilization. Smith et al. (22) showed that DGAT-1-deficient mice are lean and resistent to diet-induced obesity. Recently, it has been shown that GPAM knockout mice have reduced weight and reduced gonadal WAT mass (23). Ablation of PEPCK gene expression in WAT by disruption of the PPAR-responsive element in the PEPCK promoter reduced adipose tissue size and fat content (24). The authors also showed that adipose tissue pieces from these mice released higher amounts of NEFA. Conversely, PEPCK overexpression in mice resulted in adiposity and increased esterification of NEFA, suggesting that delivery of glycerol-3-phosphate via the PEPCK pathway is implicated in the regulation of free fatty acid mobilization (25). In cell culture studies, it was demonstrated that overexpression of GPAM enhances TG synthesis (12). Ruan and Pownall (26) showed that overexpression of LPAAT in 3T3-L1 adipocytes suppressed basal and isoproterenol-stimulated NEFA release. Other in vitro studies indicate that the enzymes responsible for GPAT, GNPAT (27, 28), and DGAT (29) are upregulated during 3T3-L1 adipocyte differentiation and hence are implicated in controlling TG synthesis in the mature adipocytes.

To test whether increased NEFA synthesis from glucose might also contribute to the cellular NEFA pool in HSL-ko mice, the rates of glucose uptake and fatty acid synthesis were determined in adipose tissue of HSL-ko mice and control animals. The uptake and accumulation of 2-deoxyglucose were decreased in HSL-deficient fat pads in tis-

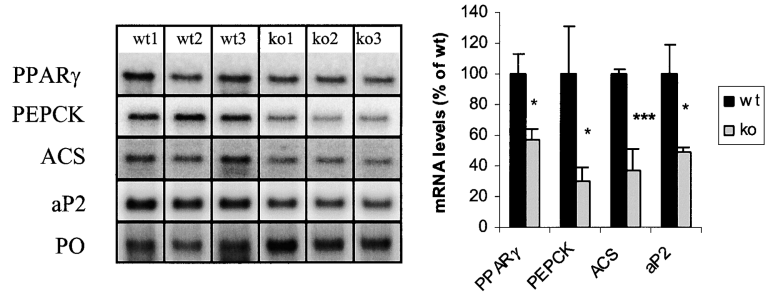

Fig. 7. Northern blotting analysis of peroxisome proliferator-activated receptor γ (PPARγ) and PPAR- regulated genes in WAT of wt and HSL-ko animals. Gonadal fat pads were surgically removed from fed mice, and total RNA (10 μg) was used for Northern blot analysis. Each lane corresponds to the RNA obtained from a single wt or HSL-ko mouse. The housekeeping gene for acidic ribosomal protein PO was used as internal standard. Northern blots were visualized by exposure to a PhosphorImager screen (Apbiotech) and analyzed using ImageQuant software. Data are expressed as means ± SD. * $P < 0.05$; *** $P < 0.001$.

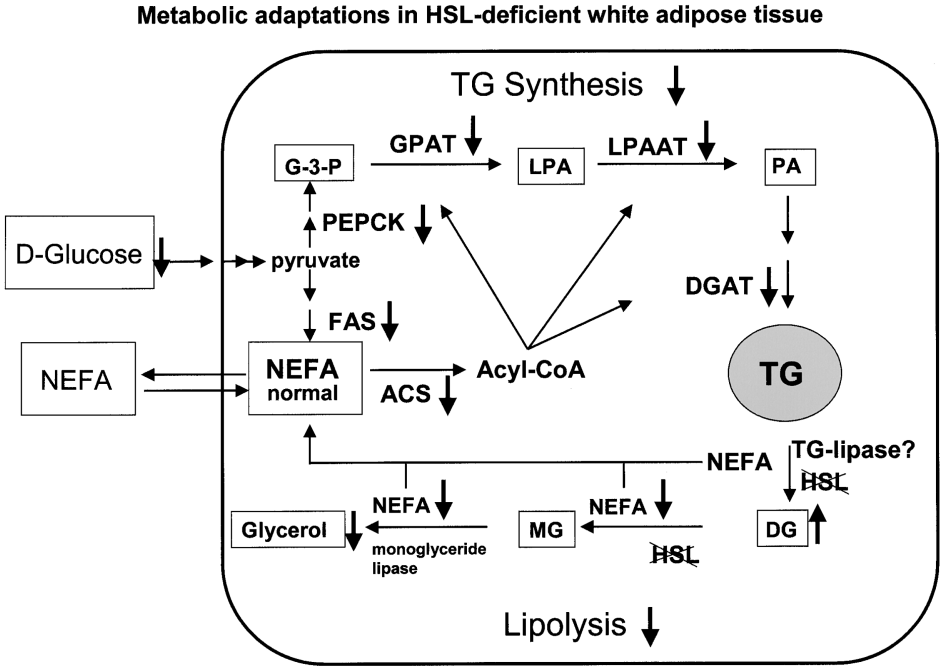

Fig. 9. In the absence of HSL, TGs are hydrolyzed to diacylglycerol (DG) by unidentified TG-lipase(s). Further hydrolysis of DG to monoglycerol (MG) is blocked, as is evident from DG accumulation and decreased release of NEFA and glycerol (5). Additionally, D-glucose uptake and fatty acid de novo synthesis are reduced in HSL-deficient WAT. Despite the decreased fatty acid production from lipolysis and de novo synthesis, normal tissue NEFA levels are maintained by a compensatory downregulation of TG synthesis. The metabolic adaptations that lead to decreased lipid synthesis include downregulation of phosphoenolpyruvate carboxykinase and acyl-CoA-synthetase, the enzymes that provide glycerol-3-phosphate (G-3-P) and acyl-CoA, respectively. Additionally, the major ATs in TG synthesis, glycerol-3-phosphate acyltransferase, LPAAT, and diacylglycerol acyltransferase, are markedly decreased. This compensatory downregulation of TG synthesis is sufficient to maintain normal cellular and plasma NEFA levels under nonfasting conditions but is not sufficient to compensate for the additional NEFA demand during prolonged fasting.

sue culture and in adipose tissue in whole-animal experiments. Additionally, the rates of fatty acid de novo synthesis as measured by the incorporation of D-glucose into fatty acids was decreased in HSL-ko mice. This was explained by decreased activities of the rate-limiting enzymes, namely ACC and FAS, in fatty acid synthesis. As a result of decreased glucose import in adipose tissue, decreased fatty acid synthesis, and decreased esterification of NEFA, the incorporation of glucose-derived carbon was markedly decreased in TGs and PLs of WAT from HSL-ko mice. These observations made it evident that the cellular NEFA pool is not fed by de novo NEFA synthesis. In fact, it is reasonable to assume that the decreased production rates of fatty acids and decreased lipid formation in HSL-deficient adipose tissue contribute to the reduction in fat mass in these animals.

To gain information about the molecular control mechanisms leading to the downregulation of fatty acid synthesis and esterification, the contribution of the transcription factors SREBP-1 and PPARγ in this process was investigated. SREBPs are synthesized as inactive precursors bound to the endoplasmatic reticulum, where they are cleaved proteolytically. The NH_2-terminal DNA binding domain (68 kDa, nSREBP) translocates to the nucleus, where it activates transcription (30). SREBP-1c stimulates the expression of many lipogenic genes, including ACC, FAS, and GPAM (30), as well as genes such as G6PDH, which deliver NADPH for the lipid synthesis pathway (31). Because expression of all of the above genes was reduced in WAT of HSL-ko mice, SREBP-1 represented an attractive candidate for the observed alterations. However, we did not find significant changes of SREBP-1 mRNA levels and nSREBP protein levels, indicating that factors other than SREBP-1 expression and proteolytic processing are responsible for the downregulation of these genes.

PPARγ is known to play a key role in adipogenesis and appears to be a master controller of the "thrifty gene response" that leads to efficient energy storage in adipocytes (32). The observed decrease of PPARγ mRNA in WAT of HSL-ko mice and the concomitant decrease in the prototypes of the PPARγ-regulated genes ACS (33), PEPCK (34), and aP2 (35) suggest that PPARγ may play an important role in this process. Additional support for an involvement of PPARγ is provided by our finding that HSL-deficient fat cells are smaller than adipocytes of normal mice. Small adipocytes have also been reported in heterozygous PPARγ-ko mice (36, 37), which supports the hypothesis that the level of PPARγ expression at least partially determines fat cell size. Currently being investigated is the mechanistic link between HSL deficiency and PPARγ downregulation, including the signaling molecules in-

volved. Among other possibilities, it is conceivable that the accumulation of diacylglycerol (DG) in HSL-deficient adipocytes (5) leads to alterations in the protein kinase C (PKC) pathway. For example, DG-dependent PKCs have been shown to act as negative regulators of insulin signaling through PI3K (38). Impaired insulin sensivity in HSL-ko mice was recently reported (39, 40) and might be instrumentally involved in the decreased TG synthesis in WAT of HSL-ko mice. Additionally, PI3K has been shown to directly affect PPARγ expression (41).

In summary, we have shown that lipogenic genes involved in fatty acid de novo synthesis and TG synthesis are downregulated in HSL-ko WAT, providing an explanation for the observed loss in WAT mass in HSL-ko mice. Furthermore, we suggest that the decreased TG synthesis in WAT counteracts the missing lipolytic activity in HSL-deficient WAT by preventing mobilized or internalized NEFA from (re-)esterification. This compensatory mechanism is an example illustrative of the interplay between TG synthesis and hydrolysis in the regulation of NEFA export from adipose tissue.

This work was supported by grant SFB Biomembranen F007 and projects F713 and P14309 of the Austrian Fonds zur Förderung der wissenschaftlichen Forschung.

REFERENCES

1. Yeaman, S. J., G. M. Smith, C. A. Jepson, S. L. Wood, and N. Emmison. 1994. The multifunctional role of hormone-sensitive lipase in lipid metabolism. *Adv. Enzyme Regul.* **34:** 355–370.
2. McKnight, G. S., D. E. Cummings, P. S. Amieux, M. A. Sikorski, E. P. Brandon, J. V. Planas, K. Motamed, and R. L. Idzerda. 1998. Cyclic AMP, PKA, and the physiological regulation of adiposity. *Recent Prog. Horm. Res.* **53:** 139–159.
3. Sztalryd, C., G. Xu, H. Dorward, J. T. Tansey, J. A. Contreras, A. R. Kimmel, and C. Londos. 2003. Perilipin A is essential for the translocation of hormone-sensitive lipase during lipolytic activation. *J. Cell Biol.* **161:** 1093–1103.
4. Syu, L. J., and A. R. Saltiel. 1999. Lipotransin: a novel docking protein for hormone-sensitive lipase. *Mol. Cell.* **4:** 109–115.
5. Haemmerle, G., R. Zimmermann, M. Hayn, C. Theussl, G. Waeg, E. Wagner, W. Sattler, T. M. Magin, E. F. Wagner, and R. Zechner. 2002. Hormone-sensitive lipase deficiency in mice causes diglyceride accumulation in adipose tissue, muscle, and testis. *J. Biol. Chem.* **277:** 4806–4815.
6. Haemmerle, G., R. Zimmermann, J. G. Strauss, D. Kratky, M. Riederer, G. Knipping, and R. Zechner. 2002. Hormone-sensitive lipase deficiency in mice changes the plasma lipid profile by affecting the tissue-specific expression pattern of lipoprotein lipase in adipose tissue and muscle. *J. Biol. Chem.* **277:** 12946–12952.
7. Okazaki, H., J. Osuga, Y. Tamura, N. Yahagi, S. Tomita, F. Shionoiri, Y. Iizuka, K. Ohashi, K. Harada, S. Kimura, T. Gotoda, H. Shimano, N. Yamada, and S. Ishibashi. 2002. Lipolysis in the absence of hormone-sensitive lipase: evidence for a common mechanism regulating distinct lipases. *Diabetes.* **51:** 3368–3375.
8. Osuga, J., S. Ishibashi, T. Oka, H. Yagyu, R. Tozawa, A. Fujimoto, F. Shionoiri, N. Yahagi, F. B. Kraemer, O. Tsutsumi, and N. Yamada. 2000. Targeted disruption of hormone-sensitive lipase results in male sterility and adipocyte hypertrophy, but not in obesity. *Proc. Natl. Acad. Sci. USA.* **97:** 787–792.
9. Wang, S. P., N. Laurin, J. Himms-Hagen, M. A. Rudnicki, E. Levy, M. F. Robert, L. Pan, L. Oligny, and G. A. Mitchell. 2001. The adipose tissue phenotype of hormone-sensitive lipase deficiency in mice. *Obes. Res.* **9:** 119–128.
10. Iritani, N., Y. Ikeda, and H. Kajitani. 1984. Selectivities of 1-acylglycerophosphorylcholine acyltransferase and acyl-CoA synthetase for n-3 polyunsaturated fatty acids in platelets and liver microsomes. *Biochim. Biophys. Acta.* **793:** 416–422.
11. Jones, K. M., and A. K. Hajra. 1994. Assay of dihydroxyacetone phosphate acyltransferase with 32P-labeled substrate. *Clin. Chem.* **40:** 946–947.
12. Igal, R. A., S. Wang, M. Gonzalez-Baro, and R. A. Coleman. 2001. Mitochondrial glycerol phosphate acyltransferase directs the incorporation of exogenous fatty acids into triacylglycerol. *J. Biol. Chem.* **276:** 42205–42212.
13. Eberhardt, C., P. W. Gray, and L. W. Tjoelker. 1997. Human lysophosphatidic acid acyltransferase. cDNA cloning, expression, and localization to chromosome 9q34.3. *J. Biol. Chem.* **272:** 20299–20305.
14. Folch, J., M. Lees, and G. H. Sloane Stanley. 1957. A simple method for the isolation and purification of total lipids from animal tissues. *J. Biol. Chem.* **226:** 497–509.
15. Coleman, R. A. 1992. Diacylglycerol acyltransferase and monoacylglycerol acyltransferase from liver and intestine. *Methods Enzymol.* **209:** 98–104.
16. Tanabe, T., S. Nakanishi, T. Hashimoto, H. Ogiwara, J. Nikawa, and S. Numa. 1981. Acetyl-CoA carboxylase from rat liver. *Methods Enzymol.* **71:** 5–16.
17. Nepokroeff, C. M., M. R. Lakshmanan, and J. W. Porter. 1975. Fatty-acid synthase from rat liver. *Methods Enzymol.* **35:** 37–44.
18. Labarca, C., and K. Paigen. 1980. A simple, rapid, and sensitive DNA assay procedure. *Anal. Biochem.* **102:** 344–352.
19. Sambrook, J., E. F. Fritsch, and T. Maniatis. 1989. Molecular Cloning: A Laboratory Manual. 2nd edition. Cold Spring Harbor Laboratory Press, Cold Spring Harbor, NY.
20. Kraemer, F. B., and W. J. Shen. 2002. Hormone-sensitive lipase: control of intracellular tri-(di-)acylglycerol and cholesteryl ester hydrolysis. *J. Lipid Res.* **43:** 1585–1594.
21. Kalderon, B., N. Mayorek, E. Berry, N. Zevit, and J. Bar-Tana. 2000. Fatty acid cycling in the fasting rat. *Am. J. Physiol. Endocrinol. Metab.* **279:** E221–E227.
22. Smith, S. J., S. Cases, D. R. Jensen, H. C. Chen, E. Sande, B. Tow, D. A. Sanan, J. Raber, R. H. Eckel, and R. V. Farese, Jr. 2000. Obesity resistance and multiple mechanisms of triglyceride synthesis in mice lacking Dgat. *Nat. Genet.* **25:** 87–90.
23. Hammond, L. E., P. A. Gallagher, S. Wang, S. Hiller, K. D. Kluckman, E. L. Posey-Marcos, N. Maeda, and R. A. Coleman. 2002. Mitochondrial glycerol-3-phosphate acyltransferase-deficient mice have reduced weight and liver triacylglycerol content and altered glycerolipid fatty acid composition. *Mol. Cell. Biol.* **22:** 8204–8214.
24. Olswang, Y., H. Cohen, O. Papo, H. Cassuto, C. M. Croniger, P. Hakimi, S. M. Tilghman, R. W. Hanson, and L. Reshef. 2002. A mutation in the peroxisome proliferator-activated receptor gamma-binding site in the gene for the cytosolic form of phosphoenolpyruvate carboxykinase reduces adipose tissue size and fat content in mice. *Proc. Natl. Acad. Sci. USA.* **99:** 625–630.
25. Franckhauser, S., S. Munoz, A. Pujol, A. Casellas, E. Riu, P. Otaegui, B. Su, and F. Bosch. 2002. Increased fatty acid re-esterification by PEPCK overexpression in adipose tissue leads to obesity without insulin resistance. *Diabetes.* **51:** 624–630.
26. Ruan, H., and H. J. Pownall. 2001. Overexpression of 1-acyl-glycerol-3-phosphate acyltransferase-alpha enhances lipid storage in cellular models of adipose tissue and skeletal muscle. *Diabetes.* **50:** 233–240.
27. Coleman, R. A., and R. M. Bell. 1980. Selective changes in enzymes of the sn-glycerol 3-phosphate and dihydroxyacetone-phosphate pathways of triacylglycerol biosynthesis during differentiation of 3T3–L1 preadipocytes. *J. Biol. Chem.* **255:** 7681–7687.
28. Hajra, A. K., L. K. Larkins, A. K. Das, N. Hemati, R. L. Erickson, and O. A. MacDougald. 2000. Induction of the peroxisomal glycerolipid-synthesizing enzymes during differentiation of 3T3–L1 adipocytes. Role in triacylglycerol synthesis. *J. Biol. Chem.* **275:** 9441–9446.
29. Cases, S., S. J. Smith, Y. W. Zheng, H. M. Myers, S. R. Lear, E. Sande, S. Novak, C. Collins, C. B. Welch, A. J. Lusis, S. K. Erickson, and R. V. Farese, Jr. 1998. Identification of a gene encoding an acyl CoA:diacylglycerol acyltransferase, a key enzyme in triacylglycerol synthesis. *Proc. Natl. Acad. Sci. USA.* **95:** 13018–13023.
30. Horton, J. D., J. L. Goldstein, and M. S. Brown. 2002. SREBPs: activators of the complete program of cholesterol and fatty acid synthesis in the liver. *J. Clin. Invest.* **109:** 1125–1131.
31. Shimomura, I., H. Shimano, B. S. Korn, Y. Bashmakov, and J. D. Horton. 1998. Nuclear sterol regulatory element-binding proteins

activate genes responsible for the entire program of unsaturated fatty acid biosynthesis in transgenic mouse liver. *J. Biol. Chem.* **273:** 35299–35306.
32. Auwerx, J. 1999. PPARgamma, the ultimate thrifty gene. *Diabetologia.* **42:** 1033–1049.
33. Schoonjans, K., B. Staels, P. Grimaldi, and J. Auwerx. 1993. Acyl-CoA synthetase mRNA expression is controlled by fibric-acid derivatives, feeding and liver proliferation. *Eur. J. Biochem.* **216:** 615–622.
34. Tontonoz, P., E. Hu, J. Devine, E. G. Beale, and B. M. Spiegelman. 1995. PPAR gamma 2 regulates adipose expression of the phosphoenolpyruvate carboxykinase gene. *Mol. Cell. Biol.* **15:** 351–357.
35. Tontonoz, P., E. Hu, R. A. Graves, A. I. Budavari, and B. M. Spiegelman. 1994. mPPAR gamma 2: tissue-specific regulator of an adipocyte enhancer. *Genes Dev.* **8:** 1224–1234.
36. Rosen, E. D., P. Sarraf, A. E. Troy, G. Bradwin, K. Moore, D. S. Milstone, B. M. Spiegelman, and R. M. Mortensen. 1999. PPAR gamma is required for the differentiation of adipose tissue in vivo and in vitro. *Mol. Cell.* **4:** 611–617.
37. Kubota, N., Y. Terauchi, H. Miki, H. Tamemoto, T. Yamauchi, K. Komeda, S. Satoh, R. Nakano, C. Ishii, T. Sugiyama, K. Eto, Y. Tsubamoto, A. Okuno, K. Murakami, H. Sekihara, G. Hasegawa, M. Naito, Y. Toyoshima, S. Tanaka, K. Shiota, T. Kitamura, T. Fujita, O. Ezaki, S. Aizawa, R. Nagai, K. Tobe, S. Kimura, and T. Kadowaki. 1999. PPAR gamma mediates high-fat diet-induced adipocyte hypertrophy and insulin resistance. *Mol. Cell.* **4:** 597–609.
38. Farese, R. V. 2001. Insulin-sensitive phospholipid signaling systems and glucose transport. Update II. *Exp. Biol. Med. (Maywood).* **226:** 283–295.
39. Mulder, H., M. Sorhede-Winzell, J. A. Contreras, M. Fex, K. Strom, T. Ploug, H. Galbo, P. Arner, C. Lundberg, F. Sundler, B. Ahren, and C. Holm. 2003. Hormone-sensitive lipase null mice exhibit signs of impaired insulin sensitivity whereas insulin secretion is intact. *J. Biol. Chem.* 278**:** 36380–36388.
40. Roduit, R., P. Masiello, S. P. Wang, H. Li, G. A. Mitchell, and M. Prentki. 2001. A role for hormone-sensitive lipase in glucose-stimulated insulin secretion: a study in hormone-sensitive lipase-deficient mice. *Diabetes.* **50:** 1970–1975.
41. Watanabe, M., K. Inukai, H. Katagiri, T. Awata, Y. Oka, and S. Katayama. 2003. Regulation of PPAR gamma transcriptional activity in 3T3–L1 adipocytes. *Biochem. Biophys. Res. Commun.* **300:** 429–436.